# *Electronic Supplementary Information to* DFTB investigations of the electronic and magnetic properties of fluorographene with vacancies and with adsorbed chemical groups

Taoufik Sakhraoui*and František Karlický†

Department of Physics, Faculty of Science, University of Ostrava, 701 03 Ostrava, Czech Republic

## Contents



*taoufik.sakhraoui@osu.cz
†frantisek.karlicky@osu.cz

# 1 Supercell Model of Fluorographene

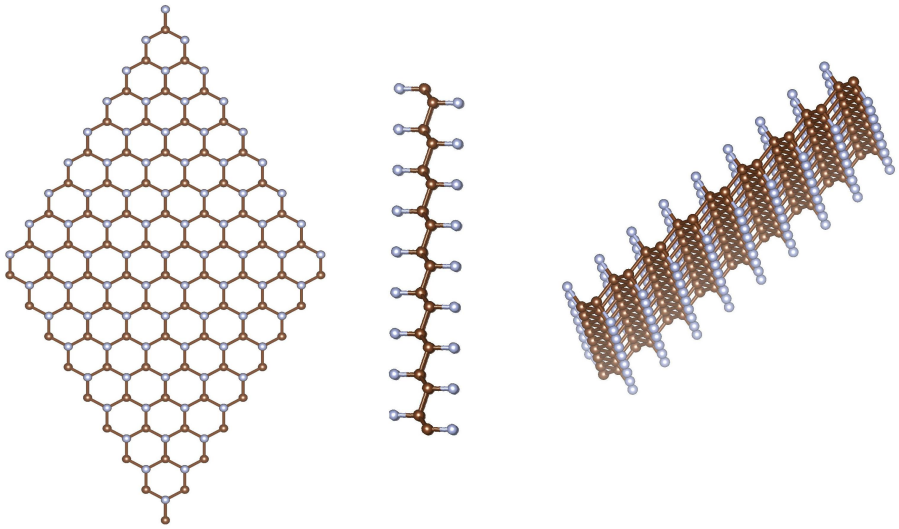

Figure S1: Different views of 9×9 pure CF supercell used in the present study. F atoms are bound to each C atom of graphene alternatingly from the top and bottom sides.

# 2 Formation Energies

The formation energy of neutral F vacancies ($E_f$) is defined as:

$$E_f = \frac{E_{tot.}(CF + Fvacancies) + n \times \mu_F - E_{tot.}(pristineCF)}{n},$$

where $E_{tot.}$(CF+Fvacancies) is the total energy of fluorographene (CF) in the presence of F vacancies, $\mu_F$ is the chemical potential of the F atom which is obtained from the converged total energy of an isolated $F_2$ molecule placed in a large cell, n is the number of F vacancies in the structure and $E_{tot.}$(pristine CF) the total energy of pure CF.

Table S1: Formation energies of different F-vacancies defect in CF.

| Concentration of F-vacancy | Formation energy (eV) |
|---|---|
| monovacancy | 5.28 |
| trivacancies | 5.32 |
| line | 5.38 |
| big cluster | 5.36 |
| armchair | 5.35 |
| zigzag | 5.33 |

## 3 Spin Densities and Density of States

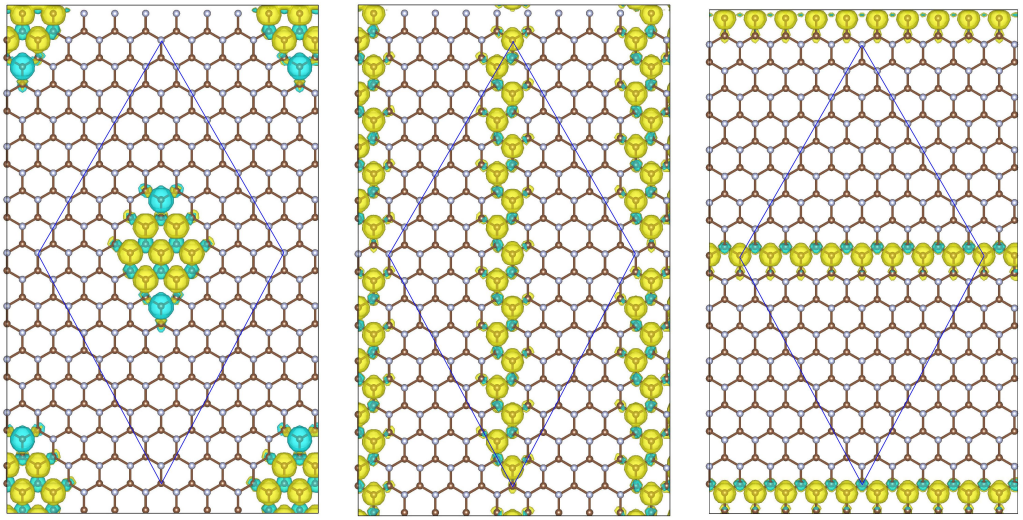


Figure S2: Spin densities distribution with isosurface = $\pm 1 \times 10^{-3}$ atomic units of (a) big cluster, (b) armchair and (c) zigzag defects using a $9 \times 9$ supercell for CF. Yellow and blue indicate positive and negative isosurfaces, respectively. Supercells are depicted in blue lines.

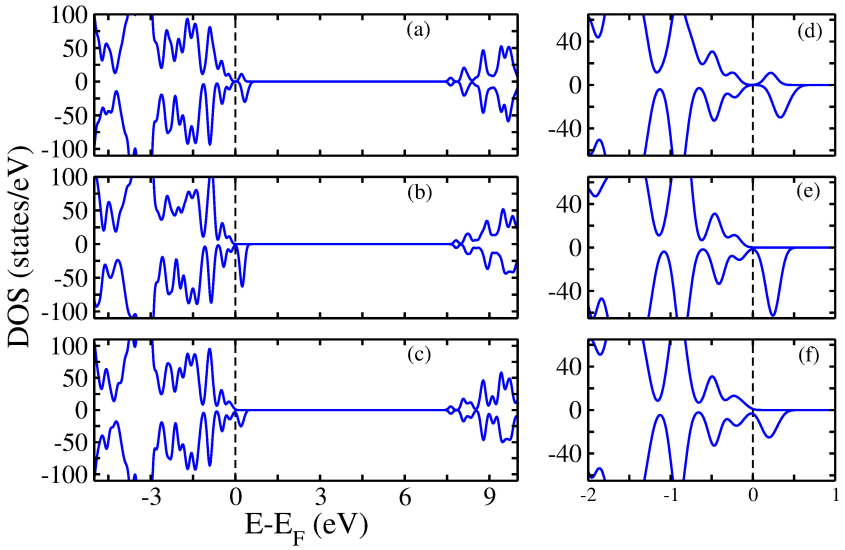


Figure S3: Electronic density of states of (a) big cluster, (b) armchair, and (d) zigzag defects. (d), (e) and (f) are zoom in the vicinity of the Fermi level. 9×9 CF supercells were used in all calculations.

# 4 Comparison of DFTB and DFT for Two F-vacancies in CF

Table S2: Relative energies of CF containing two F-vacancies in various positions (for ring labels, see Figure 5 of the main text). Direct comparison of 5×5 supercell used in DFTB and DFT[a] is performed, zero energy corresponds to the energy of the most favorable configuration.

| | DFTB | | | DFT | | |
|---|---|---|---|---|---|---|
| Ring no. | NM | FM | AFM | NM | FM | AFM |
| 1 (ortho) | 0.00 | 3.17 | – | 0.00 | 2.71 | — |
| 2 (meta) | 3.43 | 2.99 | 2.93 | 2.78 | 2.37 | 2.30 |
| 3 (para) | 3.33 | 2.92 | 2.91 | 2.97 | 2.31 | 2.29 |

[a] The spin-polarized DFT level of theory in periodic boundary conditions together with the projector augmented-wave (PAW) [Blöchl(1994), Kresse and Joubert(1999)] method as implemented in the Vienna *ab initio* Simulation Package (VASP)[Kresse and Joubert(1999)] was used. Numerical details: PBE density functional, 3×3×1 k-point grid, the cut-off energy of 400 eV for the plane-wave basis set, the break condition for the electronic step is an energy difference of $1\times10^{-6}$ eV, criterion on forces for optimization is 0.01 eV/Å.

## 5 Defluorination Path

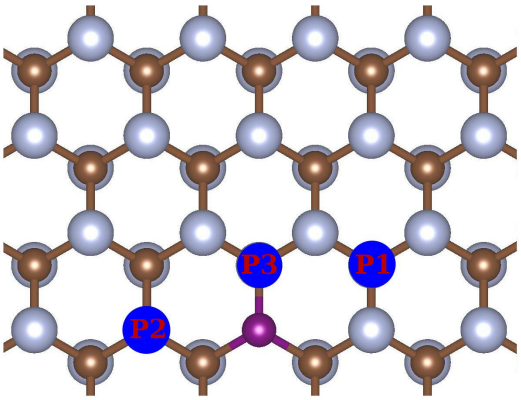


(a) interacting single F-vacancy with F-vacancy ($C_{162}F_{160}$)

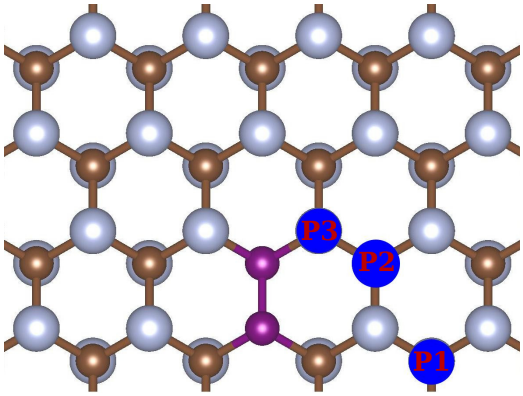


(b) interacting double F-vacancies with F-vacancy ($C_{162}F_{159}$)

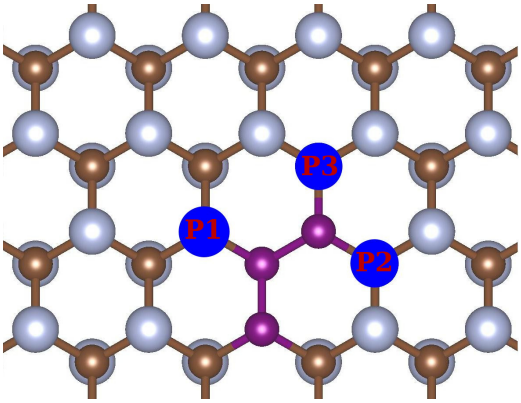


(c) interacting three F-vacancies with F-vacancy ($C_{162}F_{158}$)

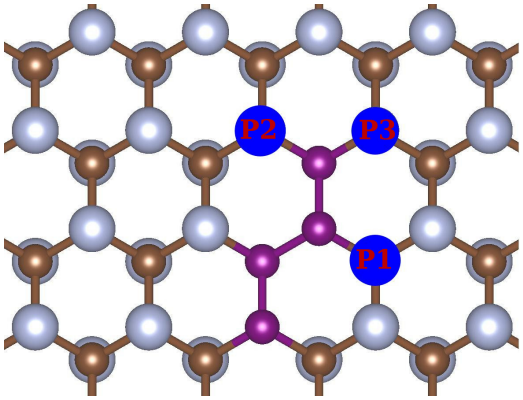


(d) interacting four F-vacancies with F-vacancy ($C_{162}F_{157}$)

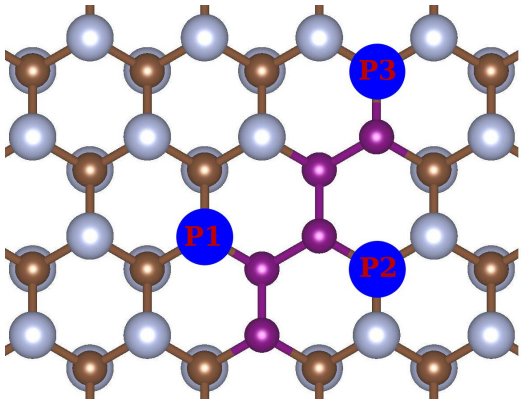


(e) interacting five F-vacancies with F-vacancy ($C_{162}F_{156}$)

Figure S4: Different possibilities for the defluorination path. (a) two F-vacancies, (b) three F-vacancies, (c) four F-vacancies, (d) five F-vacancies and (e) six F-vacancies on CF. P1, P2, and P3 refer to the first, second, and third possibilities for the introduced F-vacancy, respectively.

Table S3: Total energies ($E_T$) in eV and total magnetic moments ($M_T$) in $\mu_B$ for some possible spin orientation for 2, 3, 4, 5 and 6 F-vacancies on fluorographene. P1, P2, and P3 refer to the first, second, and third possibility for the introduced F-vacancy, respectively, as shown in detail in Supplementary Figure S4. P3 (the zigzag-direction) is the most stable position for all configurations.

| | P1 | | P2 | | P3 (zigzag) | |
|---|---|---|---|---|---|---|
| initial spin orientation | $E_T$ | $M_T$ | $E_T$ | $M_T$ | $E_T$ | $M_T$ |
| **2 F-vacancies on CF** | | | | | | |
| ↑ ↑ | -26639.2699 | 2.00 | -26639.2624 | 2.00 | -26642.1798 | NM |
| ↑ ↓ | -26639.2734 | AM | -26639.2526 | AM | -26642.1743 | NM |
| ↑ - | -26639.0098 | 0.99 | -26638.9957 | 0.98 | -26642.1778 | NM |
| **3 F-vacancies on CF** | | | | | | |
| ↑ ↑ ↑ | -26521.3920 | NM | -26521.6149 | 1.00 | -26522.3625 | 1.00 |
| ↑ ↑ ↓ | -26521.3920 | NM | -26521.6148 | 1.00 | -26522.3625 | 1.00 |
| ↑ ↓ ↑ | -26521.3920 | NM | -26521.6176 | 1.00 | -26522.3675 | 1.00 |
| - ↑ - | -26521.3969 | NM | -26521.3499 | NM | -26522.3675 | 1.00 |
| - - ↑ | -26521.3916 | NM | -26521.6087 | 1.00 | -26522.3675 | 1.00 |
| ↑ ↓ - | -26521.3916 | NM | -26521.3534 | 1.00 | -26522.3625 | 1.00 |
| ↑ - ↑ | -26521.3915 | NM | -26521.6160 | 1.00 | -26522.3675 | 1.00 |
| ↑ - ↓ | -26521.3915 | NM | -26521.6160 | 1.00 | -26522.3675 | 1.00 |
| **4 F-vacancies on CF** | | | | | | |
| ↑ ↑ ↑ ↑ | -26402.3579 | 1.99 | -26404.1995 | NM | -26404.2692 | NM |
| ↑ ↑ ↑ ↓ | -26402.0768 | 0.65 | -26404.2023 | NM | -26404.2711 | NM |
| ↑ ↑ ↓ ↓ | -26402.0853 | 0.65 | -26404.1995 | NM | -26404.2692 | NM |
| ↑ ↓ ↑ ↓ | -26402.0768 | 0.65 | -26404.1995 | NM | -26404.2692 | NM |
| ↑ ↓ - - | -26402.0852 | 0.65 | -26404.2029 | NM | -26404.2711 | NM |
| - ↑ ↑ - | -26402.0852 | 0.65 | -26404.1995 | NM | -26404.2692 | NM |
| - ↑ ↓ - | -26402.0768 | 0.65 | -26404.1995 | NM | -26404.2692 | NM |
| ↑ - - - | -26401.9308 | NM | -26404.2009 | NM | -26404.2692 | NM |
| ↑ - - ↓ | -26402.0768 | AM | -26404.1995 | NM | -26404.2692 | NM |
| ↑ - - ↑ | -26402.1730 | 0.65 | -26404.1995 | NM | -26404.2692 | NM |
| **5 F-vacancies on CF** | | | | | | |
| ↑ ↑ ↑ ↑ ↑ | -26284.3435 | 1.00 | -26284.6649 | 1.00 | -26284.7267 | 1.00 |
| ↑ ↑ ↑ ↑ ↓ | -26284.3365 | 1.00 | -26284.6649 | 1.00 | -26284.7267 | 1.00 |
| ↑ ↑ ↑ ↓ ↓ | -26284.3365 | 1.00 | -26284.6649 | 1.00 | -26284.7267 | 1.00 |
| ↑ ↑ ↓ ↑ ↑ | -26284.3365 | 1.00 | -26284.6649 | 1.00 | -26284.7247 | 1.00 |
| ↑ ↑ ↓ ↓ ↑ | -26284.3365 | 1.00 | -26284.6660 | 1.00 | -26284.7267 | 1.00 |
| ↓ ↑ ↑ ↑ ↓ | -26284.1731 | 1.00 | -26284.6649 | 1.00 | -26284.7267 | 1.00 |
| ↑ ↓ ↑ ↓ ↑ | -26284.3365 | 1.00 | -26284.6660 | 1.00 | -26284.7267 | 1.00 |
| - - ↑ ↓ - | -26284.3365 | 1.00 | -26284.6659 | 1.00 | -26284.7267 | 1.00 |
| ↑ - - - - | -26284.3365 | 1.00 | -26284.6649 | 1.00 | -26284.7267 | 1.00 |
| - - ↑ - - | -26284.3365 | 1.00 | -26284.6660 | 1.00 | -26284.7267 | 1.00 |
| ↑ ↓ - - - | -26284.3365 | 1.00 | -26284.6649 | 1.00 | -26284.7267 | 1.00 |
| - - ↑ ↑ - | -26284.3365 | 1.00 | -26284.5431 | NM | -26284.6050 | NM |
| ↑ - - - ↓ | -26284.3365 | 1.00 | -26284.5431 | NM | -26284.6013 | NM |
| - ↑ - ↓ - | -26284.3365 | 1.00 | -26284.5430 | NM | -26284.6042 | NM |
| **6 F-vacancies on CF** | | | | | | |
| ↑ ↑ ↑ ↑ ↑ ↑ | -26164.6313 | AM | -26166.2058 | NM | -26166.4234 | NM |
| ↑ ↑ ↑ ↑ ↑ ↓ | -26164.6338 | AM | -26166.2058 | NM | -26166.4233 | NM |
| ↑ ↑ ↑ ↑ ↓ ↓ | -26164.6273 | AM | -26166.2058 | NM | -26166.4234 | NM |
| ↑ ↑ ↓ ↓ ↑ ↑ | -26164.6322 | AM | -26166.2058 | NM | -26166.4233 | NM |
| ↓ ↑ ↑ ↑ ↑ ↓ | -26164.6317 | AM | -26166.2058 | NM | -26166.4233 | NM |

Continued on next page

**Table S3 – continued ...**

| | P1 | | P2 | | P3 (zigzag) | |
|---|---|---|---|---|---|---|
| initial spin orientation | $E_T$ | $M_T$ | $E_T$ | $M_T$ | $E_T$ | $M_T$ |
| ↑ ↑ ↑ ↓ ↓ ↓ | -26164.7436 | AM | -26166.2956 | NM | -26166.4233 | NM |
| ↑ ↓ ↑ ↓ ↑ ↓ | -26164.7436 | 1.99 | -26166.2058 | NM | -26166.4233 | NM |
| ↑ ↑ ↓ ↓ ↓ ↑ | -26164.5132 | 0.79 | -26166.2056 | NM | -26166.4233 | NM |
| - - ↑ ↓ - - | -26164.5132 | 0.79 | -26166.2058 | NM | -26166.4233 | NM |
| - - ↑ ↑ - - | -26164.3980 | NM | -26166.2058 | NM | -26166.4233 | NM |
| ↑ - - - - - | -26164.5584 | 0.70 | -26166.2058 | NM | -26166.4233 | NM |
| ↑ - - - - ↑ | -26164.5550 | 0.70 | -26166.2058 | NM | -26166.4234 | NM |
| ↑ ↓ - - - - | -26164.5557 | 0.70 | -26166.2058 | NM | -26166.4233 | NM |
| ↑ - - - - ↓ | -26164.5521 | 0.70 | -26166.2058 | NM | -26166.4233 | NM |

## 6 Ferrimagnetic Zigzag Chains

Table S4: Magnetic moments (in $\mu_B$) on C atoms in zigzag chains of vacancies in CF (from three to nine F-vacancies, see Figure S5 and main Figure 11). Direct comparison of 9×9 supercell used in DFTB and 7×7 supercell used in PBE DFT[a] is performed. In the DFT case, approximate magnetic moments from the projection of the (occupied) wavefunctions onto spherical harmonics were renormalized to the accurate total magnetic moment of the supercell.

| no. vac | method | $C_1$ | $C_2$ | $C_3$ | $C_4$ | $C_5$ | $C_6$ | $C_7$ | $C_8$ | $C_9$ |
|---|---|---|---|---|---|---|---|---|---|---|
| 3 | DFTB | 0.54 | -0.11 | 0.54 | | | | | | |
| | DFT | 0.48 | -0.15 | 0.48 | | | | | | |
| 5 | DFTB | 0.37 | -0.08 | 0.43 | -0.08 | 0.37 | | | | |
| | DFT | 0.35 | -0.12 | 0.39 | -0.12 | 0.35 | | | | |
| 7 | DFTB | 0.26 | -0.06 | 0.34 | -0.08 | 0.34 | -0.06 | 0.26 | | |
| | DFT | 0.27 | -0.10 | 0.32 | -0.12 | 0.32 | -0.10 | 0.27 | | |
| 9 | DFTB | 0.20 | -0.05 | 0.27 | -0.07 | 0.30 | -0.07 | 0.27 | -0.05 | 0.20 |
| | DFT | 0.22 | -0.08 | 0.27 | -0.11 | 0.29 | -0.11 | 0.27 | -0.08 | 0.22 |

[a] See Table S2 for DFT method.

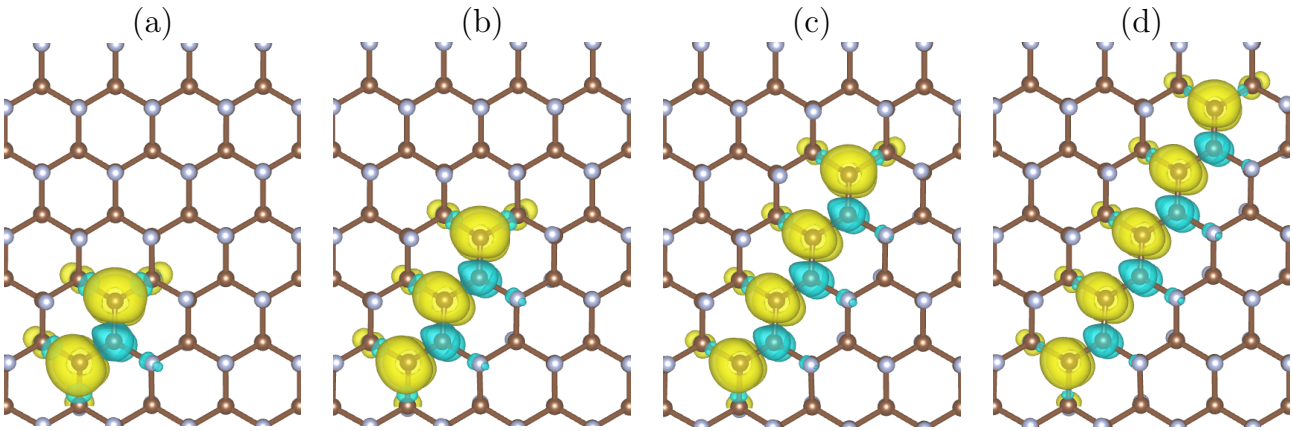


Figure S5: Spin density surfaces (cyan and yellow for up and down spin, respectively) in ferrimagnetic zigzag chains of F vacancies in CF (from 3 to 9 empty C-sites in chains, see panels (a)-(d), respectively) from PBE DFT (corresponding to Table S4).

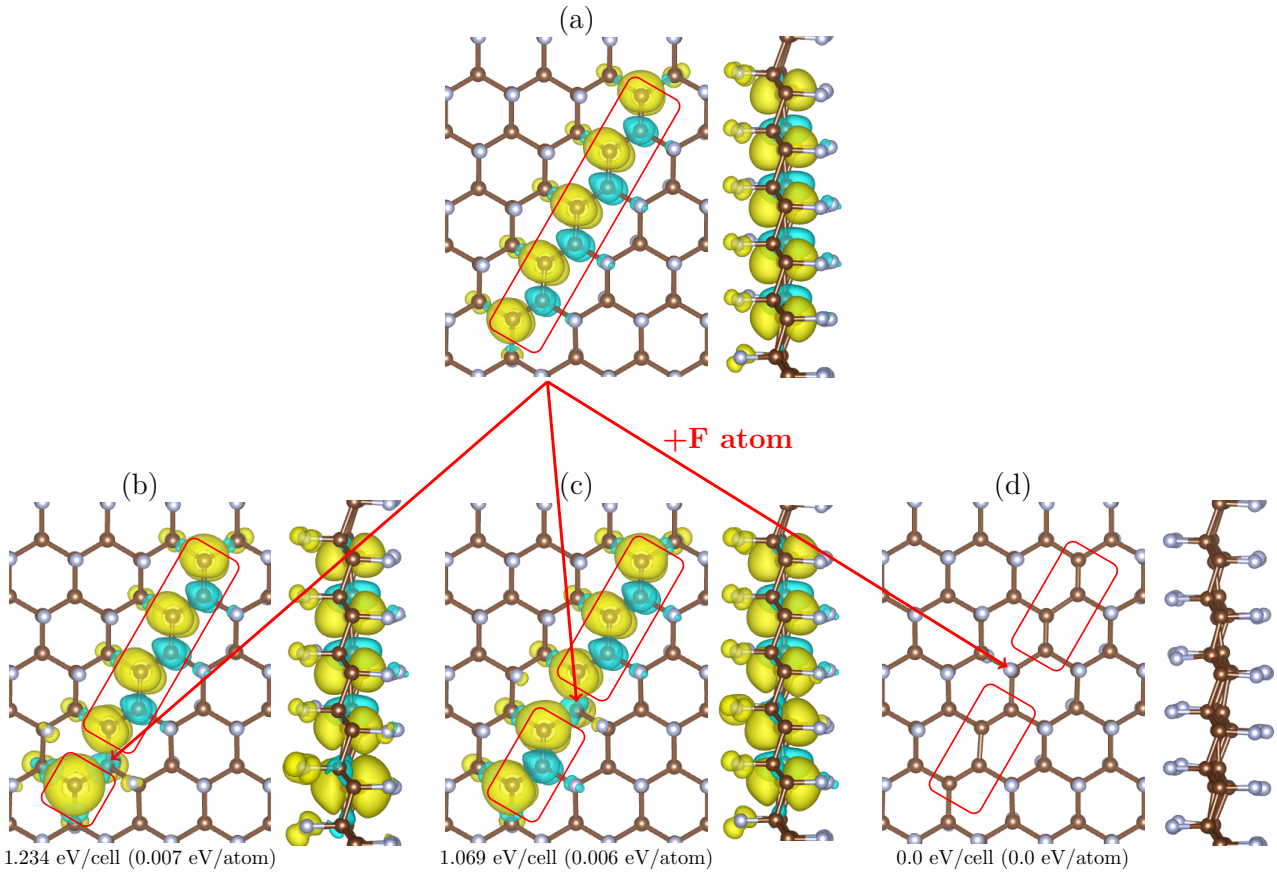


Figure S6: The zigzag chain composed of 9 F-vacancies (a) is attacked by one fluorine atom (b-c). Examples of absorption to second (b), fourth (c), and fifth (d) C atom of the chain (from the bottom) are considered. While in (b) and (c) cases two ferrimagnetic sub-chains with an odd number of magnetic C-sites are visible (the total magnetic moment of the supercell is $2\mu_B$), in (d) case two nonmagnetic sub-chains with an even number of C-sites is the result. The corresponding spin density surfaces are shown (cyan and yellow for up and down spin, respectively). Note that (d) case is energetically preferred over (b) and (c): relative energies from DFT (setup from Table S4) are reported under subfigures (zero energy corresponds to the energy of the most favorable (d) case).

## References

[Blöchl(1994)] P. E. Blöchl, *Phys. Rev. B*, 1994, **50**, 17953–17979.

[Kresse and Joubert(1999)] G. Kresse and D. Joubert, *Phys. Rev. B*, 1999, **59**, 1758–1775.